J Clin Densitom. Author manuscript; available in PMC 2016 November 02.

Published in final edited form as:

J Clin Densitom. 2015 ; 18(3): 408–418. doi:10.1016/j.jocd.2014.07.003.

A Trimodality Comparison of Volumetric Bone Imaging Technologies. Part III: SD, SEE, LSC Association With Fragility Fractures

Andy K. O. Wong[1,*], **Karen A. Beattie**[1], **Kevin K. H. Min**[2], **Zamir Merali**[3], **Colin E. Webber**[4], **Christopher L. Gordon**[5], **Alexandra Papaioannou**[6], **Angela M. W. Cheung**[7], and **Jonathan D. Adachi**[1]

[1]Department of Medicine, McMaster University, Hamilton, ON, Canada

[2]Health Sciences, McMaster University, Hamilton, ON, Canada

[3]Department of Medicine, University Health Network, Toronto, ON, Canada

[4]Department of Nuclear Medicine, Hamilton Health Sciences, Hamilton, ON, Canada

[5]Department of Nuclear Medicine, McMaster University, Hamilton, ON, Canada

[6]Division of Geriatrics, Hamilton Health Sciences, Hamilton, ON, Canada

[7]Osteoporosis Program, University Health Network, Toronto, ON, Canada

Abstract

Part II of this 3-part series demonstrated 1-yr precision, standard error of the estimate, and 1-yr least significant change for volumetric bone outcomes determined using peripheral (p) quantitative computed tomography (QCT) and peripheral magnetic resonance imaging (pMRI) modalities in vivo. However, no clinically relevant outcomes have been linked to these measures of change. This study examined 97 women with mean age of 75 ± 9 yr and body mass index of 26.84 ± 4.77 kg/m^2, demonstrating a lack of association between fragility fractures and standard deviation, least significant change and standard error of the estimate-based unit differences in volumetric bone outcomes derived from both pMRI and pQCT. Only cortical volumetric bone mineral density and cortical thickness derived from high-resolution pQCT images were associated with an increased odds for fractures. The same measures obtained by pQCT erred toward significance. Despite the smaller 1-yr and short-term precision error for measures at the tibia vs the radius, the associations with fractures observed at the radius were larger than at the tibia for high-resolution pQCT. Unit differences in cortical thickness and cortical volumetric bone mineral density able to yield a 50% increase in odds for fractures were quantified here and suggested as a reference for future power computations.

Keywords

Clinical sensitivity; fragility fractures; least significant change; pMRI; pQCT

[*]Address correspondence to: Andy K.O. Wong, PhD, Department of Medicine, McMaster University, 501-25 Charlton Ave E, Hamilton, ON, Canada L8N 1Y2. wongko@mcmaster.ca.

Introduction

The previous reports in this 3-part trimodality comparison highlighted the acceptable short-term precision errors for volumetric bone outcomes derived from high-resolution (HR) peripheral quantitative computed tomography (pQCT) followed by pQCT, and then 1.0 T peripheral magnetic resonance images (pMRI) (REF1). In addition, the same pattern of long-term precision error was demonstrated, whereas exclusion of individuals with a history of fragility fractures or who were current antiresorptive users resulted in smaller long-term precision error for pQCT and pMRI (REF2). With the exception of trabecular number (Tb.N), all apparent trabecular microstructural measurements were shown to be valid as compared with HR-pQCT (REF1). However, the challenge associated with the measurements of change detectability (standard error of the estimate [SEE]) and clinically least significant change (LSC) is that there have been, so far, no associations drawn between these statistics and an actual clinical endpoint. Consequently, it remains unknown to what degree a given change in each volumetric outcome is associated with fragility fractures. The classical method of describing sensitivity involves the measurement of change in response per unit change in stimulus. This slope definition could be addressed by evaluating the association between given unit changes in each volumetric bone outcome and corresponding increases in the risk for fragility fractures. A base statistical model without any covariates would best describe this measurement. Although a number of studies have reported odds ratios (ORs) or hazard ratios (HRs) demonstrating the association between volumetric bone outcomes and fragility fractures, most studies targeted the goal of estimating fracture risk and not the goal of quantifying clinical sensitivity. An extrapolation of the magnitude of change in volumetric bone outcome required to achieve a standardized effect size (i.e., 50% increase in fracture risk) would be informative of the comparative clinical sensitivity across different techniques.

Most studies measuring odds and risks for fractures do not actually relate change in bone outcomes with fractures. Instead, the notion of change is represented by the associated increased odds or risks per unit difference in the outcome (interpreted as a hypothetical increase or decrease). Laib et al (1) demonstrated that each standard deviation (SD) increase in HR-pQCT-derived trabecular spacing (Tb.Sp), and decrease in Tb.N was associated with an age-adjusted increase of 1.85–2.03-fold in the odds for fractures. However, in a similar cross-sectional analysis, Melton et al (2) did not see any association between volumetric bone outcomes and prevalent fractures at the distal radius using HR-pQCT images. Although not examined in terms of changes in SDs, MacIn-tyre et al (3) showed that pQCT-derived mean intertrabecular hole area greater than 2 SDs from the mean translated to a 5.4-fold increase in the odds for fractures. One investigation by Boutry et al (4) reported a significantly increased odds for fractures per SD difference in 11 of 13 volumetric bone outcomes obtained from calcaneous scans on MRI. All the aforementioned studies only quantified bone at a single point in time and adjusted for a number of covariates.

The present study therefore juxtaposed the clinical sensitivity of volumetric bone outcomes derived from HR-pQCT, pQCT, and 1.0 T pMRI by quantifying the odds for fragility fractures associated with each unit decrease or increase in volumetric bone measure expressed as SD, LSC, or SEE units. This investigation also extrapolated these associations

to determine the specific volumetric bone outcome values at which at least a 50% increase in the odds for fragility fractures would be observed.

This trimodality comparison is presented as the final component of a 3-part series discussing intermodality differences in technological limitations vs advantages in volumetric bone imaging.

Methods

This observational cohort study quantified volumetric bone outcome values derived from HR-pQCT, pQCT, and 1.0 T pMRI images, as well as retrospectively associated these outcomes with a history of fragility fractures. All study procedures were completed within 3.5 yr. Women 50 yr and older enrolled in the Canadian Multicentre Osteoporosis Study (CaMOS) and living within a 50 km radius of the Hamilton (Ontario, Canada) CaMOS site were considered eligible to participate (N = 340). CaMOS is an ongoing prospective cohort study of community-dwelling randomly selected women and men 25 yr and older at 9 major Canadian cities. The main CaMOS objectives, methodology, and sampling framework are described in detail elsewhere (5). Participants were randomly selected from all eligible women from the Hamilton CaMOS cohort. Women with valid contraindications to MRI (pacemaker, insulin pumps) were excluded. Those participants weighing above 250 lbs were excluded from HR-pQCT and 1.0 T pMRI procedures because of the weight limit of the positioning chair. Women with self-reported tremors were also excluded to avoid significant motion artifact.

Participants volunteered in the completion of a pQCT, HR-pQCT, and 1.0 T pMRI ultradistal radius scan at baseline and at 1 yr follow-up. Repeated imaging was also performed at the ultradistal tibia for pQCT and HR-pQCT. One-yr repeats of these imaging procedures enabled the computation of long-term precision statistics with which fragility fractures were associated. Details of each imaging procedure have been reported in part I of this series. Because of limitations in the gantry diameter and depth, ultradistal tibia scans were not completed using pMRI. A complete list of current medications including dose, duration, and frequency, was collected at study visit. Information on medical conditions and ascertained incident fragility fractures from the last 15 yr was obtained from the CaMOS database. Fragility fractures were defined as nontraumatic fractures occurring as the result of a fall from standing height or less, excluding any fractures of the skull, fingers, and toes.

All study procedures were overseen and approved by the St. Joseph’s Healthcare Research Ethics Board in Hamilton and the University Health Network in Toronto (Ontario, Canada).

High-Resolution Peripheral Quantitative Computed Tomography

Scans were performed at the ultradistal radius and tibia at the standard regions of interest (ROIs) using the same imaging parameters as previously described (REF1) for the HR-pQCT (XtremeCT v1; Scanco Medical AG, Bassersdorf, Switzerland). After acquiring 110 transaxial computed tomographic slices at an isotropic voxel resolution of 82 μm, acceptable quality images (grade 3 motion and below (6)) were semiautomatically segmented using Scanco software (Scanco Medical AG, Bassersdorf, Switzerland) and computed for apparent

microstructural outcomes (bone volume/total volume [BV/TV], Tb.Sp, trabecular thickness [Tb.Th], Tb.N, cortical thickness [Ct.Th], integral, cortical, and trabecular volumetric bone mineral density [vBMD], subscripts: i, c, tr). Hydroxyapatite rod phantoms were scanned daily for quality control purposes.

Peripheral Quantitative Computed Tomography

Ultradistal radius and tibia scans were performed using an XCT2000 model pQCT (Stratec, Pforzheim, Germany) at an ROI coinciding with that of HR-pQCT. Two slices, each 2.5 ± 0.3 mm thick, were obtained 11.5 mm and 16.5 mm proximal to the radial tilt midpoint; and 24.5 mm and 29.5 mm proximal to the tibial end plate plateau, at an in-plane resolution of 200 μm (REF1). Hydroxyapatite phantoms were assessed on days in which scans were obtained. Only images with no discontinuities in the cortical bone were accepted for image analyses. Densitometric ($vBMD_i$, $vBMD_c$, $vBMD_{tr}$) measures were computed using Stratec v5.2.1 software (Stratec, Pforzheim, Germany); apparent trabecular microstructure (Tb.Sp, BV/TV, Tb.N, Tb.Th) and Ct.Th were computed with custom software package, pQCT OsteoQ (Inglis Software Solutions, Inc, Hamilton, Ontario, Canada).

1.0 T Peripheral MRI

Ultradistal radius scans at the same 9.5 mm ROI as HR-pQCT were performed on a 1.0 T pMRI OrthOne scanner (GE Healthcare, Pittsburgh, PA, USA). A series of 20 slices in tandem, each 1.0 mm thick, was prescribed perpendicular to the long axis of the radius using a T_1-weighted spoiled 3D gradient recalled echo sequence (SPGR) yielding an in-plane resolution of 195 μm (REF1). A geometric phantom was assessed on days in which scans were obtained. Only images that preserved sufficient sharpness and trabecular textural pattern were accepted for image analyses. Trabecular apparent structural outcomes (Tb.Sp, BV/TV, Tb.N, and Tb.Th) were obtained from the central 18 slices using a custom-designed software package, MRI OsteoQ (Inglis Software Solutions, Inc, Hamilton, Ontario, Canada) on a per-slice basis and averaged to yield a final measure.

Volumetric Bone Outcome Computation

All volumetric bone outcomes were derived from equations previously reported for HR-pQCT (7) and histomorphometry. The latter was based on Parfitt's model of parallel plates and derived from single slices (8)—hereon forward termed "model-dependent" outcomes. The former was not based on Parfitt's model, but on equations assuming analysis of a volume.

Data Analyses

All long-term precision statistics including LSC and SEE were referenced from part II of this series (REF2). Analyses were performed on all baseline variables. Binary logistics regression models were fit to volumetric bone outcome data derived from each modality, reporting OR and corresponding 95% confidence intervals (CIs) expressed per unit SD, LSC, or SEE increase or decrease in volumetric bone outcome—the directionality was dependent on the expected increased odds for fractures. All models were examined with only a single volumetric bone outcome as an exogenous variable. Secondary models

included only age as a covariate. Significant ($p < 0.05$) or marginally significant associations ($p < 0.10$) were further examined by graphing the relationship between the magnitude of volumetric bone outcome increase or decrease and the consequential increase in odds for fragility fractures. A 50% increase in odds (OR: 1.5) for a fragility fracture was considered a benchmark for clinical significance. 95% confidence intervals were estimated around each OR of 1.5. Specific differences in volumetric bone outcome values achieving this benchmark were reported by extrapolating based on logistic regression equations.

Results

In total, 97 study participants completed at least 1 set of baseline procedures on 1 or more imaging modalities. Among these participants, 59 of 97 (60.8%) who had a MRI, 32 of 56 (57.1%) who had a pQCT scan, and 40 of 68 (58.8%) who had a HR-pQCT scan—all respectively had a history of fragility fractures. As described in part II of this series, at least 59 participants completed 1 set of baseline and follow-up scans, allowing the calculation of LSC and SEE values associated with each modality-specific volumetric bone outcome (REF2). Women in the fractured group were older and were on antiresorptive therapy for a longer duration than those who have not sustained a fragility fracture. All other characteristics were balanced between fractured and nonfractured groups (Table 1). None of the participants were on long-term glucocorticoid therapy, had undergone any organ transplant, had primary or secondary hyper- or hypoparathyroidism, or had recently been immobilized because of injury.

Clinical Sensitivity: Disease Odds

Neither pMRI images nor pQCT images yielded any bone outcomes that were significantly associated with fragility fractures (Tables 2, 3 and 4). For HR-pQCT, decrease in Ct.Th by an amount equivalent to the SD, LSC, or SEE at the radius and tibia was associated with increases between 6% and 85% in the odds for a fragility fracture. Similarly, 1 SD, LSC, or SEE unit decrease in cortical vBMD was associated with up to 3-fold increase in the odds for a fragility fracture (Table 5). Although MRI did not generate any cortical measurements, pQCT-derived Ct.Th at the radius and tibia both showed ORs over 1.10 with CIs erring toward 1.00, but did not reach significance. The similar case was true for cortical vBMD at the tibia but not at the radius (Tables 3 and 4). Radius and tibia differences in fracture odds were apparent for most measures. For example, 1 unit decrease in the LSC for HR-pQCT-derived Ct.Th was associated with a 45% increase in the odds for a fragility fracture at the radius, but only 13% increase for Ct.Th obtained at the tibia.

Threshold for Yielding at Least 50% Increase in Odds for Fractures

For HR-pQCT, the amount of Ct.Th difference at the tibia that would translate to as much as a 50% increase in the odds for fractures was exactly double the difference required at the radius. For cortical vBMD, the magnitude of difference required to yield a 50% increase in the odds for fractures was comparable between the radius and tibia (Table 6). Age appeared to make little impact on the amount of difference in bone outcome measures required to translate to an OR of 1.50 for fragility fractures. Although regression models were not significant for pQCT-derived bone outcome measures, the magnitude of difference required

for an OR of 1.50 was displayed for comparison, showing much larger differences required to demonstrate a 50% increase in the odds for fractures than for HR-pQCT.

Discussion

Summary of Results

In the local cohort of women with mean age 75 ± 9 yr and body mass index 26.84 ± 4.77 kg/m^2, neither pMRI nor pQCT yielded any volumetric bone outcomes that demonstrated an increased odds for fragility fractures. However, pQCT did reveal evidence toward an OR larger than 1.0 with CIs just undershooting 1.0. Both Ct.Th and cortical vBMD outcomes were the primary candidates for fracture associations for HR-pQCT. ORs were largest when expressed per unit SD difference in the volumetric bone outcome in question. This study presented significant ORs even with a smaller sample size for HR-pQCT. Differences in Ct.Th and cortical vBMD that were able to yield a 50% increase in odds for fractures were treated as a benchmark for a clinically significant difference threshold.

Clinical Sensitivity: Odds for Fractures

The fact that neither pMRI nor pQCT yielded any bone outcomes that showed associations with fractures could be due to the lack of statistical power given the larger 1-yr precision error of measurements compared with HR-pQCT. Even with HR-pQCT, only Ct.Th and vBMD, but not other volumetric bone outcomes, showed increases in odds for fragility fractures. Although not significant, pQCT-derived Ct.Th and vBMD demonstrated a trend toward increased odds for fractures per SD, LSC, or SEE unit decrease in Ct.Th, suggesting that cortical measures bear an important effect size for fracture associations. Because of the varying magnitudes of SD, SEE, and LSC units, the ORs yielded were noticeably different. In particular, the detection limit measure, SEE, showed the lowest OR. Although LSC comprises an element of precision error measured by root mean square SDs, expression of odds per SD difference in the measurement across individuals generated a larger OR than LSC, which accounts only for within-individual variation. The interpretation of the OR from each case can be put into context: (1) increased odds for fractures per lowest unit change detectable by the instrument (SEE), (2) increased odds for fractures per lowest unit of intraindividual clinically meaningful change (LSC), and (3) increased odds for fractures per standardized unit of interindividual variability (SD). Although the first contextual example references a property of the machine (detection limit) and can be comparable across individuals, it lacks a clinical rationale. Thus, translation of this knowledge into practice may not immediately make sense to physicians and patients. Contextual example 2 provides a clearer reference to the patient, but intraindividual change may be sensitive to cohort effects. The LSC for different study populations may need to be quantified. The third contextual example considers interindividual differences but when the population examined becomes highly diverse, the meaning of the unit of SD may be more difficult to interpret. Because LSC and SDs are simply population statistics with fixed values, the odds for fractures for both scenarios could be compared in making the final interpretation of fracture odds.

A number of studies have examined the association between volumetric bone apparent microstructural outcomes and fractures using HR-pQCT at the radius (2,9–16) and tibia (10,13–16). However, only few have investigated the same using either pQCT (3,17–19) or MRI (1,20–23). Other studies determined the association between vBMD derived from pQCT images and spinal (HRs or ORs: 1.1–1.9) (18,24–26), hip (HRs or ORs: 1.1–2.6) (24,26,27), or wrist (ORs: 0.51–1.87) (3) fractures, but these studies did not examine apparent bone microstructure. In general, 1 SD difference in apparent bone microstructural outcomes derived from HR-pQCT, pQCT, or MRI were able to yield increased odds for fractures between 1.32 and 5.38 at the ultradistal radius site, with an average OR across studies for all bone outcomes of 2.24. ORs at the ultradistal tibia ranged from 1.28 to 3.70 with a mean of 1.65 across studies. These mean effect sizes were in the same order of magnitude as ORs yielded from HR-pQCT volumetric bone microstructural outcomes reported from the present study. However, caution must be taken in comparing ORs across studies because of variable imaging conditions applied (most importantly: type of modality, exact ROI localization, and resolution). One analysis by Cortet et al (22) in women (mean age: 69 ± 10 yr) demonstrated significant associations between MRI-derived bone outcomes and fractures, but acknowledged the fact that fewer outcomes were significant compared with HR-pQCT performed on the same study participants. Majumdar et al (21) also observed nonsignificant ORs for microstructural outcomes. However, when their ROI was expanded from 1 to 3 cm, there were significant differences observed between fractured and nonfractured groups. Sornay-Rendu et al (13) measured a larger OR for Ct.Th at the distal radius compared with the present study using HR-pQCT. This larger effect size could be explained by the fact that this group limited fractures to radiologically confirmed vertebral fractures. With the exception of Tb.N, all other bone outcomes that Szulc et al (14) and Sheu et al (19) examined demonstrated ORs similar to those reported by HR-pQCT and pQCT at both radius and tibia, although they focused on men.

Threshold for Yielding at Least 50% Increase in Odds for Fractures

This is the first report of using a binary logistic regression model to generate a clinically significant value that corresponds with a fixed benchmark for clinical significance (50% increased odds for fractures). The threshold difference in volumetric bone outcomes can be easily interpreted and can be applied to future sample size calculations where the notion of “desirable change” is often sought with limited guidance. This measurement further addresses the limitation of the LSC, a distribution-based method that only interprets clinical significance as effect sizes that are represented by values 1.96 SDs away from the mean, adjusted by the number of measurements (28). Certainly, the limitations of a binary logistic regression model extend to the interpretation of this 50% increased odds threshold for representing change. For reflecting the error surrounding this threshold estimate, it is advisable to report the 95% CI surrounding the targeted OR of 1.50. The choice of 50% was arbitrary and could be advisable, as modeled by the Delphi method (29), by a panel of experts after receipt of a larger study demonstrating prospective association between said bone outcomes and fractures.

Study Limitations

The OR computed from binary logistic regression analysis is based on cross-sectional data and therefore is subject to questions about whether causation can be implied. However, when the rate of events such as fragility fractures is low, the OR closely approximates the HR, a statistic that estimates the risk of future fractures (30). It is possible that individuals who have previously sustained a fragility fracture, depending on the anatomical location, may suffer from reduced mobility, further leading to disuse osteoporosis. This condition may most likely be relevant for individuals who have recently had a fracture rather than those who experienced one a greater number of years ago. The present study did not adjust for time since last fracture, which could have improved the gradient of risk estimated. Also, fractures were not subcategorized into type, location, clinical, or subclinical. Although this investigation focused on peripheral ROIs, their relevance to the location of major osteoporotic fractures such as the hip and spine remain questioned.

Liu et al (31) showed a correlation between tibial integral vBMD obtained by HR-pQCT and stiffness of the proximal femur ($r = 0.75$). Similarly, vertebral stiffness was correlated with trabecular vBMD of the distal radius ($r = 0.58$). One study by Horikoshi et al (32) saw trabecular and cortical vBMD correlations between the femoral neck and distal radius ($r =$ 0.639, 0.517, and 0.351, respectively) using the XCT3000 model of pQCT. Despite the smaller sample size used to examine odds for fractures in the local study sample, there were no major model fit issues.

Recommendations

Although pQCT-derived volumetric bone outcomes previously demonstrated a high degree of reproducibility and smaller 1-yr change compared with pMRI, its association with fractures remains smaller than HR-pQCT-derived outcomes. It is recommended that HR-pQCT be used primarily for studies requiring higher sensitivity to changes. Here, it was demonstrated that Ct.Th and cortical vBMD were the most clinically relevant outcomes to use. In fact, the data suggest that Ct.Th and vBMD measurements obtained at the radius may be more sensitive than the same measurement at the tibia, in terms of any association with fractures. However, the short- and long-term precision errors for radius measures are larger than the tibia, necessitating larger sample sizes to observe the same effect. Caution must be exercised when considering pQCT-derived volumetric bone outcomes for longitudinal studies. When computing sample sizes for longitudinal studies, it is recommended that the aforementioned difference thresholds yielding 50% increased odds for fractures be used. If other magnitudes of fracture associations are desired, the graphs in Figs. 1 and 2 could be used. As larger studies evaluating prospective fracture risk are performed, more accurate thresholds for clinically significant change can be reported using the same methods.

Acknowledgments

This three-part series is dedicated to Dr. Colin E. Webber. Andy Kin On Wong was funded by a Vanier CGS Doctoral Award at the time of this project (CGV-104858). All CaMOS participants are thanked for their dedication and over a decade of volunteerism. The CaMOS study staff are thanked for overseeing the operation of the parent CaMOS study.

References

1. Laib A, Newitt DC, Lu Y, Majumdar S. New model-independent measures of trabecular bone structure applied to in vivo high-resolution MR images. Osteoporos Int. 2002; 13(2):130–136. [PubMed: 11905523]
2. Melton LJ 3rd, Riggs BL, Keaveny TM, et al. Structural determinants of vertebral fracture risk. J Bone Miner Res. 2007; 22(12):1885–1892. [PubMed: 17680721]
3. MacIntyre NJ, Adachi JD, Webber CE. In vivo measurement of apparent trabecular bone structure of the radius in women with low bone density discriminates patients with recent wrist fracture from those without fracture. J Clin Densitom. 2003; 6(1):35–43. [PubMed: 12665700]
4. Boutry N, Cortet B, Dubois P, et al. Trabecular bone structure of the calcaneus: preliminary in vivo MR imaging assessment in men with osteoporosis. Radiology. 2003; 227(3):708–717. [PubMed: 12676974]
5. Kreiger N, Tenenhouse A, Joseph L, et al. Research notes: the Canadian Multicentre Osteoporosis Study (CaMos)—background, rationale, methods. Can J Aging. 1999; 18(3):12.
6. Pauchard Y, Liphardt AM, Macdonald HM, et al. Quality control for bone quality parameters affected by subject motion in high-resolution peripheral quantitative computed tomography. Bone. 2012; 50(6):1304–1310. [PubMed: 22445540]
7. Laib A, Ruegsegger P. Calibration of trabecular bone structure measurements of in vivo three-dimensional peripheral quantitative computed tomography with 28-microm-resolution microcomputed tomography. Bone. 1999; 24(1):35–39. [PubMed: 9916782]
8. Parfitt AM, Mathews CH, Villanueva AR, et al. Relationships between surface, volume, and thickness of iliac trabecular bone in aging and in osteoporosis. Implications for the microanatomic and cellular mechanisms of bone loss. J Clin Invest. 1983; 72(4):1396–1409. [PubMed: 6630513]
9. Melton LJ 3rd, Riggs BL, van Lenthe GH, et al. Contribution of in vivo structural measurements and load/strength ratios to the determination of forearm fracture risk in postmenopausal women. J Bone Miner Res. 2007; 22(9):1442–1448. [PubMed: 17539738]
10. Vico L, Zouch M, Amirouche A, et al. High-resolution pQCT analysis at the distal radius and tibia discriminates patients with recent wrist and femoral neck fractures. J Bone Miner Res. 2008; 23(11):1741–1750. [PubMed: 18665795]
11. Boutroy S, Van Rietbergen B, Sornay-Rendu E, et al. Finite element analysis based on in vivo HR-pQCT images of the distal radius is associated with wrist fracture in postmenopausal women. J Bone Miner Res. 2008; 23(3):392–399. [PubMed: 17997712]
12. Sornay-Rendu E, Boutroy S, Munoz F, Delmas PD. Alterations of cortical and trabecular architecture are associated with fractures in postmenopausal women, partially independent of decreased BMD measured by DXA: the OFELY study. J Bone Miner Res. 2007; 22(3):425–433. [PubMed: 17181395]
13. Sornay-Rendu E, Cabrera-Bravo JL, Boutroy S, et al. Severity of vertebral fractures is associated with alterations of cortical architecture in postmenopausal women. J Bone Miner Res. 2009; 24(4): 737–743. [PubMed: 19113929]
14. Szulc P, Boutroy S, Vilayphiou N, et al. Cross-sectional analysis of the association between fragility fractures and bone microarchitecture in older men: the STRAMBO study. J Bone Miner Res. 2011; 26(6):1358–1367. [PubMed: 21611974]
15. Vilayphiou N, Boutroy S, Szulc P, et al. Finite element analysis performed on radius and tibia HR-pQCT images and fragility fractures at all sites in men. J Bone Miner Res. 2011; 26(5):965–973. [PubMed: 21541999]
16. Cejka D, Patsch JM, Weber M, et al. Bone microarchitecture in hemodialysis patients assessed by HR-pQCT. Clin J Am Soc Nephrol. 2011; 6(9):2264–2271. [PubMed: 21737853]
17. Jamal SA, Gilbert J, Gordon C, Bauer DC. Cortical pQCT measures are associated with fractures in dialysis patients. J Bone Miner Res. 2006; 21(4):543–548. [PubMed: 16598374]
18. Gorai I, Nonaka K, Kishimoto H, et al. Cut-off values determined for vertebral fracture by peripheral quantitative computed tomography in Japanese women. Osteoporos Int. 2001; 12(9): 741–748. [PubMed: 11605740]

19. Sheu Y, Zmuda JM, Boudreau RM, et al. Bone strength measured by peripheral quantitative computed tomography and the risk of nonvertebral fractures: the osteoporotic fractures in men (MrOS) study. J Bone Miner Res. 2011; 26(1):63–71. [PubMed: 20593412]
20. Link TM, Majumdar S, Augat P, et al. In vivo high resolution MRI of the calcaneus: differences in trabecular structure in osteoporosis patients. J Bone Miner Res. 1998; 13(7):1175–1182. [PubMed: 9661082]
21. Majumdar S, Link TM, Augat P, et al. Trabecular bone architecture in the distal radius using magnetic resonance imaging in subjects with fractures of the proximal femur. Magnetic Resonance Science Center and Osteoporosis and Arthritis Research Group. Osteoporos Int. 1999; 10(3):231–239. [PubMed: 10525716]
22. Cortet B, Boutry N, Dubois P, et al. In vivo comparison between computed tomography and magnetic resonance image analysis of the distal radius in the assessment of osteoporosis. J Clin Densitom. 2000; 3(1):15–26. [PubMed: 10917740]
23. Chang G, Honig S, Liu Y, et al. 7 Tesla MRI of bone microarchitecture discriminates between women without and with fragility fractures who do not differ by bone mineral density. J Bone Miner Metab. 2014 (in press).
24. Formica CA, Nieves JW, Cosman F, et al. Comparative assessment of bone mineral measurements using dual X-ray absorptiometry and peripheral quantitative computed tomography. Osteoporos Int. 1998; 8(5):460–467. [PubMed: 9850355]
25. Grampp S, Genant HK, Mathur A, et al. Comparisons of noninvasive bone mineral measurements in assessing age-related loss, fracture discrimination, and diagnostic classification. J Bone Miner Res. 1997; 12(5):697–711. [PubMed: 9144335]
26. Clowes JA, Eastell R, Peel NF. The discriminative ability of peripheral and axial bone measurements to identify proximal femoral, vertebral, distal forearm and proximal humeral fractures: a case control study. Osteoporos Int. 2005; 16(12):1794–1802. [PubMed: 15947861]
27. Augat P, Fan B, Lane NE, et al. Assessment of bone mineral at appendicular sites in females with fractures of the proximal femur. Bone. 1998; 22(4):395–402. [PubMed: 9556141]
28. Hangartner TN. A study of the long-term precision of dual-energy X-ray absorptiometry bone densitometers and implications for the validity of the least-significant-change calculation. Osteoporos Int. 2007; 18(4):513–523. [PubMed: 17136486]
29. Wyrwich KW, Fihn SD, Tierney WM, et al. Clinically important changes in health-related quality of life for patients with chronic obstructive pulmonary disease: an expert consensus panel report. J Gen Intern Med. 2003; 18(3):196–202. [PubMed: 12648251]
30. Symons MJ, Moore DT. Hazard rate ratio and prospective epidemiological studies. J Clin Epidemiol. 2002; 55(9):893–899. [PubMed: 12393077]
31. Liu XS, Cohen A, Shane E, et al. Bone density, geometry, microstructure, and stiffness: relationships between peripheral and central skeletal sites assessed by DXA, HR-pQCT, and cQCT in premenopausal women. J Bone Miner Res. 2010; 25(10):2229–2238. [PubMed: 20499344]
32. Horikoshi T, Endo N, Uchiyama T, et al. Peripheral quantitative computed tomography of the femoral neck in 60 Japanese women. Calcif Tissue Int. 1999; 65(6):447–453. [PubMed: 10594163]

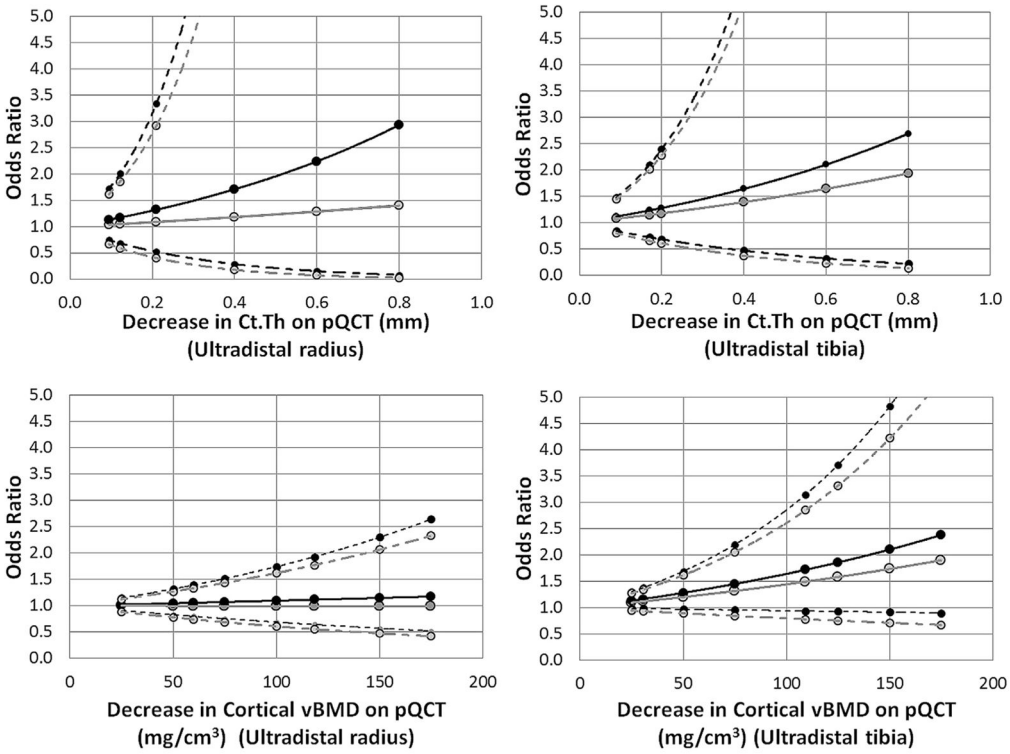

Fig. 1.

Odds for fragility fractures associated with different magnitudes of pQCT bone variable differences. Odds ratios were computed from binary logistic regression models for different values of Ct.Th (top) and cortical vBMD (bottom) as obtained using high-resolution peripheral quantitative computed tomography images of the radius (left) and tibia (right). Dashed lines represent 95% confidence intervals. Black lines and points represent base models, and gray lines and points represent models after adjustment for age. Ct.Th, cortical thickness; pQCT, peripheral quantitative computed tomography; vBMD, volumetric bone mineral density.

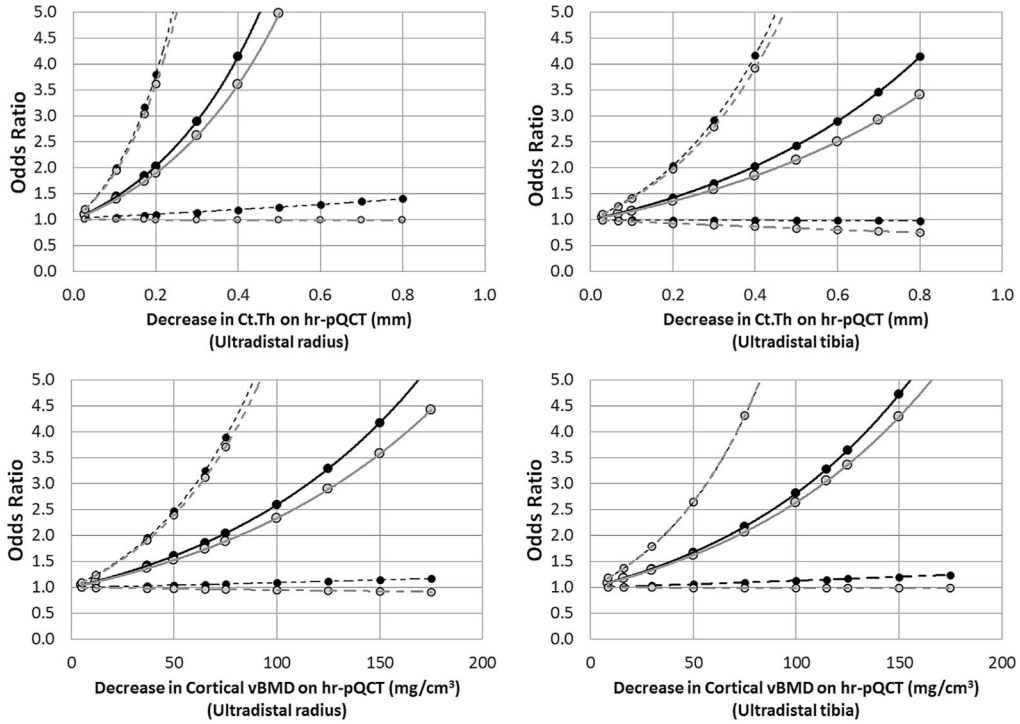

Fig. 2.

Odds for fragility fractures associated with different magnitudes of HR-pQCT bone. Odds ratios were computed from binary logistic regression models for different values of Ct.Th (top) and cortical vBMD (bottom) as obtained using HR-pQCT images of the radius (left) and tibia (right). Dashed lines represent 95% confidence intervals. Black lines and points represent base models, and gray lines and points represent models after adjustment for age. Ct.Th, cortical thickness; HR-pQCT, high-resolution peripheral quantitative computed tomography; vBMD, volumetric bone mineral density.

Table 1

Participant Characteristics at Baseline Between Fractured and Nonfractured Groups

	No fractures		History of fractures		
Variable	**Mean[a]/median[b]**	**SD[a]/Q1–Q3[b]**	**Mean[a]/median[b]**	**SD[a]/Q1–Q3[b]**	***p* Value for group comparison**
Age (yr)[a]	71	8	76	10	0.014
BMI (kg/m^2)[a]	27.31	5.80	27.72	5.71	0.727
Weight (kg)[a]	67.7	18.4	70.3	13.4	0.416
Height (m)[a]	1.56	0.26	1.60	0.07	0.351
Calcium (yr)[b]	5.0	0.0–12.0	5.5	0.0–14.0	0.712
Vitamin D_3 (yr)[b]	2.8	0.0–12.0	5.5	1.5–12.0	0.408
Antiresorptives (yr)[b]	0.0	0.0–0.0	0.0	0.0–5.0	0.036

Note: Anthropometrics and medication use descriptive statistics for study participants completing at least baseline and follow-up scans for any of the imaging modalities are displayed in the table.

Abbr: BMI, body mass index; SD, standard deviation.

[a]Parametric variable described using mean and SDs.

[b]Nonparametric variable characterized by median and first (Q1) and third (Q3) quartiles.

Table 2

pMRI Radius Bone Variables' Association With Fragility Fractures

	Unadjusted			Age-adjusted		
Bone variable	**OR (CI) per SD**	**OR (CI) per LSC**	**OR (CI) per SEE**	**OR (CI) per SD**	**OR (CI) per LSC**	**OR (CI) per SEE**
BV/TV (fraction)	1.04 (0.69, 1.58)	1.04 (0.69, 1.58)	1.02 (0.88, 1.18)	0.94 (0.61, 1.46)	0.94 (0.61, 1.45)	0.98 (0.84, 1.14)
Tb.Sp (mm)	1.17 (0.75, 1.82)	1.08 (0.87, 1.33)	1.03 (0.95, 1.12)	1.07 (0.67, 1.70)	1.03 (0.82, 1.29)	1.01 (0.93, 1.10)
Tb.Sp MI (mm)	1.16 (0.75, 1.80)	1.09 (0.85, 1.40)	1.04 (0.94, 1.14)	1.06 (0.66, 1.68)	1.03 (0.79, 1.35)	1.01 (0.91, 1.12)
Tb.Th (mm)	0.67 (0.43, 1.05)	0.31 (0.08, 1.16)	0.61 (0.35, 1.07)	0.63 (0.39, 1.03)	0.26 (0.06, 1.08)	0.57 (0.31, 1.03)
Tb.Th MI (mm)	0.70 (0.45, 1.08)	0.34 (0.09, 1.26)	0.64 (0.36, 1.10)	0.66 (0.41, 1.06)	0.29 (0.07, 1.17)	0.59 (0.33, 1.07)
Tb.N (no./mm)	1.25 (0.81, 1.92)	1.32 (0.77, 2.28)	1.13 (0.89, 1.42)	1.18 (0.75, 1.86)	1.23 (0.69, 2.19)	1.09 (0.85, 1.40)

Note: Magnitude of fracture odds associated with each SD, LSC, or SEE increase (+) or decrease (−) in radius bone variables obtained from pMRI was determined using a binary logistic regression model. Models were examined with and without adjusting for age. CI = 95% CI (lower, upper).

Abbr: BV/TV, bone volume/total volume; CI, confidence interval; LSC, least significant change; MI, Model-Independent; OR, odds ratio; pMRI, peripheral magnetic resonance imaging; SD, standard deviation; SEE, standard error of the estimate; Tb.N, trabecular number; Tb.Sp, trabecular spacing; Tb.Th, trabecular thickness.

Table 3

pQCT Radius Bone Variables' Association With Fragility Fractures

	Unadjusted			Age-adjusted		
Bone variable	**OR (CI) per SD**	**OR (CI) per LSC**	**OR (CI) per SEE**	**OR (CI) per SD**	**OR (CI) per LSC**	**OR (CI) per SEE**
BV/TV (fraction)	0.91 (0.53, 1.56)	0.96 (0.75, 1.22)	0.98 (0.88, 1.10)	0.84 (0.48, 1.48)	0.92 (0.72, 1.19)	0.96 (0.86, 1.08)
Tb.Sp (mm)	1.08 (0.63, 1.86)	1.03 (0.85, 1.24)	1.01 (0.94, 1.09)	0.96 (0.54, 1.72)	0.99 (0.81, 1.20)	1.00 (0.92, 1.08)
Tb.Sp MI (mm)	1.08 (0.63, 1.86)	1.03 (0.85, 1.24)	1.01 (0.94, 1.09)	0.96 (0.54, 1.72)	0.99 (0.81, 1.20)	1.00 (0.92, 1.08)
Tb.Th (mm)	0.64 (0.36, 1.15)	0.67 (0.39, 1.13)	0.81 (0.62, 1.07)	0.66 (0.36, 1.18)	0.68 (0.40, 1.16)	0.82 (0.62, 1.08)
Tb.Th MI (mm)	0.64 (0.36, 1.15)	0.67 (0.39, 1.13)	0.81 (0.62, 1.07)	0.66 (0.36, 1.18)	0.68 (0.40, 1.16)	0.82 (0.62, 1.08)
Tb.N (no./mm)	1.18 (0.68, 2.03)	1.11 (0.79, 1.55)	1.05 (0.89, 1.25)	1.04 (0.58, 1.86)	1.03 (0.71, 1.47)	1.01 (0.84, 1.21)
Ct.Th (mm)	1.18 (0.69, 2.02)	1.33 (0.53, 3.35)	1.14 (0.75, 1.73)	1.05 (0.60, 1.86)	1.09 (0.41, 2.92)	1.04 (0.67, 1.62)
$vBMD_i$ (mg/cm^3)	0.98 (0.56, 1.68)	0.97 (0.55, 1.74)	0.99 (0.77, 1.26)	0.90 (0.51, 1.59)	0.89 (0.49, 1.64)	0.95 (0.74, 1.23)
$vBMD_c$ (mg/cm^3)	1.12 (0.64, 1.93)	1.17 (0.53, 2.59)	1.06 (0.80, 1.39)	0.99 (0.56, 1.77)	0.99 (0.43, 2.29)	1.00 (0.74, 1.34)
$vBMD_{tr}$ (mg/cm^3)	0.67 (0.38, 1.19)	0.69 (0.40, 1.18)	0.79 (0.57, 1.11)	0.69 (0.38, 1.24)	0.71 (0.41, 1.22)	0.81 (0.57, 1.13)

Note: Magnitude of odds for fragility fractures associated with each SD, LSC, or SEE increase (+) or decrease (−) in radius bone variables obtained from pQCT images was determined with a binary logistic regression model. Models were examined with and without adjusting for age. CI = 95% CI (lower, upper).

Abbr: Ct.Th, cortical thickness; BV/TV, bone volume/total volume; CI, confidence interval; LSC, least significant change; MI, Model-Independent; OR, odds ratio; pQCT, peripheral quantitative computed tomography; SD, standard deviation; SEE, standard error of the estimate; Tb.N, trabecular number; Tb.Sp, trabecular spacing; Tb.Th, trabecular thickness; $vBMD_C$, cortical volumetric bone mineral density; $vBMD_i$, integral volumetric bone mineral density; $vBMD_{tr}$, trabecular volumetric bone mineral density.

Table 4

pQCT Tibia Bone Variables' Association With Fragility Fractures

	Unadjusted			Age-adjusted		
Bone variable	**OR (CI) per SD**	**OR (CI) per LSC**	**OR (CI) per SEE**	**OR (CI) per SD**	**OR (CI) per LSC**	**OR (CI) per SEE**
BV/TV (fraction)	0.94 (0.55, 1.60)	0.97 (0.78, 1.22)	0.99 (0.91, 1.07)	0.88 (0.50, 1.54)	0.95 (0.75, 1.20)	0.98 (0.90, 1.07)
Tb.Sp (mm)	1.10 (0.63, 1.90)	1.03 (0.85, 1.26)	1.01 (0.96, 1.06)	0.98 (0.55, 1.77)	1.00 (0.81, 1.23)	1.00 (0.94, 1.06)
Tb.Sp MI (mm)	1.10 (0.63, 1.90)	1.03 (0.85, 1.26)	1.01 (0.96, 1.06)	0.98 (0.55, 1.77)	0.99 (0.80, 1.23)	1.00 (0.94, 1.06)
Tb.Th (mm)	0.79 (0.46, 1.36)	0.84 (0.56, 1.26)	0.93 (0.79, 1.10)	0.78 (0.44, 1.37)	0.83 (0.55, 1.26)	0.93 (0.78, 1.10)
Tb.Th MI (mm)	0.79 (0.46, 1.36)	0.84 (0.56, 1.26)	0.93 (0.79, 1.10)	0.78 (0.44, 1.37)	0.83 (0.55, 1.26)	0.93 (0.78, 1.10)
Tb.N (no./mm)	1.20 (0.69, 2.09)	1.08 (0.85, 1.39)	1.03 (0.95, 1.12)	1.11 (0.61, 2.02)	1.05 (0.80, 1.37)	1.02 (0.93, 1.11)
Ct.Th (mm)	1.24 (0.72, 2.13)	1.23 (0.73, 2.10)	1.12 (0.84, 1.48)	1.15 (0.65, 2.04)	1.15 (0.66, 2.01)	1.08 (0.80, 1.45)
$vBMD_i$ (mg/cm^3)	1.29 (0.74, 2.24)	1.13 (0.86, 1.49)	1.06 (0.94, 1.20)	1.15 (0.64, 2.06)	1.07 (0.80, 1.43)	1.03 (0.91, 1.18)
$vBMD_c$ (mg/cm^3)	1.72 (0.94, 3.14)	1.36 (0.96, 1.92)	1.16 (0.98, 1.38)	1.49 (0.78, 2.85)	1.26 (0.87, 1.82)	1.12 (0.93, 1.34)
$vBMD_{tr}$ (mg/cm^3)	0.69 (0.39, 1.22)	0.82 (0.60, 1.11)	0.90 (0.76, 1.06)	0.67 (0.37, 1.21)	0.81 (0.59, 1.11)	0.89 (0.75, 1.06)

Note: Magnitude of odds for fragility fractures associated with each SD, LSC, or SEE increase (+) or decrease (−) in tibia bone variables obtained on pQCT was determined with a binary logistic regression model. Models were examined with and without adjusting for age. CI = 95% CI (lower, upper).

Abbr: Ct.Th, cortical thickness; BV/TV, bone volume/total volume; CI, confidence interval; LSC, least significant change; MI, Model-Indpendent; OR, odds ratio; pQCT, peripheral quantitative computed tomography; SD, standard deviation; SEE, standard error of the estimate; Tb.N, trabecular number; Tb.Sp, trabecular spacing; Tb.Th, trabecular thickness; $vBMD_C$, cortical volumetric bone mineral density; $vBMD_i$, integral volumetric bone mineral density; $vBMD_{tr}$, trabecular volumetric bone mineral density.

Table 5

HR-pQCT Bone Variables' Association With Fragility Fractures

	Unadjusted			Age-adjusted		
Bone variables	**OR (CI) per SD**	**OR (CI) per LSC**	**OR (CI) per SEE**	**OR (CI) per SD**	**OR (CI) per LSC**	**OR (CI) per SEE**
Radius variable						
BV/TV (fraction)	0.90 (0.55, 1.46)	0.98 (0.90, 1.08)	0.99 (0.95, 1.04)	0.85 (0.52, 1.41)	0.97 (0.88, 1.07)	0.98 (0.94, 1.03)
Tb.Sp MI (mm)	0.88 (0.54, 1.42)	1.07 (0.84, 1.37)	1.03 (0.92, 1.15)	0.78 (0.46, 1.31)	1.13 (0.87, 1.48)	1.06 (0.94, 1.19)
Tb.Th MI (mm)	0.97 (0.59, 1.57)	0.97 (0.64, 1.47)	0.99 (0.82, 1.19)	0.99 (0.60, 1.65)	0.99 (0.64, 1.53)	1.00 (0.82, 1.21)
Tb.N (no./mm)	0.87 (0.54, 1.42)	0.88 (0.55, 1.40)	0.94 (0.76, 1.17)	0.78 (0.47, 1.31)	0.79 (0.48, 1.29)	0.90 (0.71, 1.13)
Ct.Th (mm)	**1.85 (1.08, 3.17)**	**1.45 (1.05, 2.00)**	**1.10 (1.01, 1.20)**	**1.74 (1.00, 3.04)**	**1.40 (1.00, 1.95)**	**1.09 (1.00, 1.20)**
$vBMD_i$ (mg/cm^3)	1.42 (0.86, 2.36)	1.13 (0.95, 1.35)	1.03 (0.98, 1.08)	1.33 (0.79, 2.25)	1.10 (0.92, 1.33)	1.03 (0.98, 1.08)
$vBMD_c$ (mg/cm^3)	**1.86 (1.06, 3.26)**	**1.42 (1.03, 1.96)**	**1.12 (1.01, 1.25)**	1.74 (0.97, 3.12)	1.37 (0.98, 1.91)	1.11 (0.99, 1.24)
$vBMD_{tr}$ (mg/cm^3)	0.90 (0.56, 1.47)	0.98 (0.89, 1.08)	0.99 (0.94, 1.04)	0.86 (0.52, 1.42)	0.97 (0.88, 1.07)	0.98 (0.93, 1.04)
Tibia variable						
BV/TV (fraction)	0.90 (0.55, 1.46)	0.99 (0.94, 1.04)	0.99 (0.96, 1.03)	0.84 (0.51, 1.39)	0.98 (0.94, 1.03)	0.99 (0.96, 1.02)
Tb.Sp MI (mm)	0.97 (0.60, 1.57)	1.02 (0.80, 1.29)	1.01 (0.91, 1.11)	0.89 (0.54, 1.46)	1.06 (0.83, 1.35)	1.02 (0.93, 1.13)
Tb.Th MI (mm)	1.22 (0.74, 2.01)	1.23 (0.73, 2.08)	1.10 (0.86, 1.41)	1.26 (0.75, 2.13)	1.28 (0.74, 2.21)	1.12 (0.87, 1.45)
Tb.N (no./mm)	0.87 (0.54, 1.42)	0.86 (0.51, 1.46)	0.93 (0.73, 1.19)	0.78 (0.47, 1.30)	0.76 (0.44, 1.33)	0.88 (0.68, 1.14)
Ct.Th (mm)	1.72 (0.99, 2.97)	**1.13 (1.00, 1.27)**	**1.06 (1.00, 1.11)**	1.60 (0.90, 2.84)	1.11 (0.98, 1.26)	1.05 (0.99, 1.11)
$vBMD_i$ (mg/cm^3)	1.31 (0.78, 2.20)	1.03 (0.98, 1.08)	1.01 (0.99, 1.04)	1.20 (0.69, 2.06)	1.02 (0.97, 1.07)	1.01 (0.98, 1.03)
$vBMD_c$ (mg/cm^3)	**3.28 (1.16, 9.34)**	**1.18 (1.02, 1.37)**	**1.09 (1.01, 1.18)**	3.05 (0.99, 9.39)	**1.17 (1.00, 1.37)**	**1.09 (1.00, 1.18)**
$vBMD_{tr}$ (mg/cm^3)	0.90 (0.55, 1.46)	0.99 (0.94, 1.04)	1.00 (0.98, 1.02)	0.84 (0.51, 1.39)	0.98 (0.93, 1.03)	0.99 (0.97, 1.01)

Note: Magnitude of odds for fragility fractures associated with each SD, LSC, or SEE increase (+) or decrease (−) in radius (top) and tibia (bottom) bone variables obtained from HR-pQCT images was determined with a binary logistic regression model. Models were examined with and without adjusting for age. CI = 95% CI (lower, upper). Bold indicates significant statistic at $p < 0.05$.

Abbr: Ct.Th, cortical thickness; BV/TV, bone volume/total volume; CI, confidence interval; LSC, least significant change; MI, Model-Independent; OR, odds ratio; pQCT, peripheral quantitative computed tomography; SD, standard deviation; SEE, standard error of the estimate; Tb.N, trabecular number; Tb.Sp, trabecular spacing; Tb.Th, trabecular thickness; $vBMD_C$, cortical volumetric bone mineral density; $vBMD_i$, integral volumetric bone mineral density; $vBMD_{tr}$, trabecular volumetric bone mineral density.

Table 6

Changes in Bone Variables Required to Yield 50% Increase in Odds for Fractures

Modality	Radius bone outcome	OR (95% CI)	Difference in bone outcome
HR-pQCT	Ct.Th	**1.50 (1.05, 2.14)**	**−0.114 mm**
pQCT	Ct.Th	1.50 (0.40, 5.66)	−0.301 mm
HR-pQCT	$vBMD_c$	**1.50 (1.04, 2.16)**	**−42.50 mg/cm^3**
pQCT	$vBMD_c$	1.50 (0.20, 11.52)	−440.72 mg/cm^3
Age-adjusted values			
HR-pQCT	Ct.Th	**1.50 (1.00, 2.25)**	**−0.126 mm**
pQCT	Ct.Th	1.50 (0.02, 132.07)	−0.956 mm
HR-pQCT	$vBMD_c$	1.50 (0.98, 2.30)	−47.70 mg/cm^3
pQCT	$vBMD_c$	1.50 (0.00, +N)	—
Modality	Tibia bone outcome	OR (95% CI)	Difference in bone outcome
HR-pQCT	Ct.Th	**1.50 (1.00, 2.26)**	**−0.228 mm**
pQCT	Ct.Th	1.50 (0.54, 4.17)	−0.327 mm
HR-pQCT	$vBMD_c$	**1.50 (1.05, 2.14)**	**−38.99 mg/cm^3**
pQCT	$vBMD_c$	1.50 (0.95, 2.36)	−81.91 mg/cm^3
Age-adjusted values			
HR-pQCT	Ct.Th	1.50 (0.91, 2.47)	−0.265 mm
pQCT	Ct.Th	1.50 (0.30, 7.52)	−0.490 mm
HR-pQCT	$vBMD_c$	**1.50 (1.00, 2.26)**	**−41.76 mg/cm^3**
pQCT	$vBMD_c$	1.50 (0.78, 2.88)	−110.48 mg/cm^3

Note: Logistic regression equations were used to extrapolate the magnitude of difference in Ct.Th and cortical vBMD required to yield an OR of 1.50 at the 95% confidence level for both pQCT and HR-pQCT. Values were reported separately for bone outcomes derived from the radius and tibia as well as with and without adjustment for age. Bold indicates variables that were significant at the 95% confidence level in binary logistic regression models. The symbol "—" indicates estimates that were not generated because of infinite CIs around the OR.

Abbr: CI, confidence interval; OR, odds ratio; Ct.Th, cortical thickness; HR-pQCT, high-resolution peripheral quantitative computed tomography; $vBMD_C$, cortical volumetric bone mineral density.